

See discussions, stats, and author profiles for this publication at: <https://www.researchgate.net/publication/231654420>

# Size-Dependent Optical Properties of Colloidal ZnO Nanoparticles Charged by Photoexcitation

ARTICLE in THE JOURNAL OF PHYSICAL CHEMISTRY C · DECEMBER 2009

Impact Factor: 4.77 · DOI: 10.1021/jp908879h

CITATIONS

31

READS

37

4 AUTHORS, INCLUDING:



**Oleksandr L. Stroyuk**

L.V. Pisarzhevskiy Institute Of Physical Che...

150 PUBLICATIONS 1,172 CITATIONS

SEE PROFILE



**Volodymyr Dzhagan**

National Academy of Sciences of Ukraine

96 PUBLICATIONS 583 CITATIONS

SEE PROFILE



**Vitaliy V. Shvalagin**

L.V. Pisarzhevskiy Institute Of Physical Che...

35 PUBLICATIONS 264 CITATIONS

SEE PROFILE

## Size-Dependent Optical Properties of Colloidal ZnO Nanoparticles Charged by Photoexcitation

Oleksandr L. Stroyuk,<sup>\*,†</sup> Volodymyr M. Dzhagan,<sup>‡,§</sup> Vitaliy V. Shvalagin,<sup>†</sup> and Stepan Ya. Kuchmiy<sup>†</sup>

*L. V. Pysarzhevskiy Institute of Physical Chemistry, National Academy of Science of Ukraine, Prospect Nauky 31, Kyiv 03028, Ukraine, and V. E. Lashkaryov Institute of Semiconductors Physics, National Academy of Science of Ukraine, Prospect Nauky 41, Kyiv 03028, Ukraine*

*Received: September 14, 2009; Revised Manuscript Received: November 19, 2009*

The above-bandgap illumination of colloidal ZnO nanoparticles (NPs) in ethanol solutions is found to lead to reversible shifts of the absorption and photoluminescence (PL) excitation spectra, indicating charging of the nanoparticles with electrons. A rapid drop of deep-level PL intensity at the early stage of illumination is observed simultaneously with the splitting-off and growth of a new red-shifted near-band-edge PL band. Such a splitting of the near-bandgap PL band under illumination is observed for the first time and corroborates with the previous assumptions about the behavior of the NP ensemble emission upon gradual NPs' charging with electrons. The possible relation between the new PL band and photoinduced charging of NPs with excess electrons is discussed on the basis of the dependence of the PL spectrum evolution and absorption band shift relaxation on the NP size and controllable access of oxygen during illumination.

### Introduction

Zinc oxide nanostructures have been attracting increasing interest due to their large application potential in different UV-emitting devices, spintronics, or transparent electronics.<sup>1–3</sup> A challenge, however, remains in the preparation of low-cost nanoscale ZnO materials with high crystallinity and narrow spectral photoluminescence (PL) bands of high efficiency. Typical nanocrystalline ZnO materials, such as colloidal zinc oxide nanoparticles (NPs) or nanocrystalline ZnO powders produced by the hydrothermal approach usually reveal broad luminescence bands with low quantum yields not suitable for optical applications.<sup>1–3</sup> In addition, these disadvantages make it difficult to spectrally separate different PL bands and to identify the dominant emission mechanisms at room temperature. The room-temperature recombination is still under debate and is mostly attributed to free or bound excitons and their phonon replica.<sup>2,4</sup> Therefore, much effort is currently being undertaken to elaborate an easy way of production of ZnO NPs and to thoroughly understand their electronic and optical properties. Among others tasks, the realization of a controllable (reversible) n- or p-doping of the ZnO NPs is of special application interest. In view of the fundamental problem of doping NPs by introduction of impurities,<sup>5</sup> alternative ways are considered, on the basis of the electropolarization<sup>6</sup> and optical excitation.<sup>7</sup>

In the present paper we discuss the illumination-induced transformation of the absorption and PL spectra of the series of colloidal ZnO NPs of different size in ethanol solutions. We observe an appearance of a new near-bandgap PL band and attribute it to the negatively charged NPs.

### Materials and Methods

Zinc oxide NPs were synthesized in dried ethanol by basic hydrolysis of zinc acetate (reagent grade) with sodium hydroxide (pure) at 0 °C.<sup>8</sup> After the synthesis colloidal ZnO solution was kept at 55–60 °C for 2 h. The average size of ZnO NPs was varied by increasing the precursor concentrations from  $2 \times 10^{-3}$  to  $2 \times 10^{-2}$  M.

The absorbance and PL spectra were registered with Specord 220 spectrophotometer and Perkin-Elmer LS55 luminescence spectrometer, respectively. The PL excitation wavelength was 320 nm. Illumination of colloidal solutions was carried out in air in 10.0 mm optical quartz cuvettes or after argon bubbling in sealed 10.0 mm glass cuvettes. The light source in the illumination experiments was either the xenon lamp of the luminescence spectrometer with  $\lambda = 320$  nm (the light intensity measured by ferrioxalate actinometry was  $3.3 \times 10^{15}$  quanta/min) or a high-pressure mercury lamp equipped with a combination of optical filters cutting a narrow spectral region of 310–370 nm ( $1.6 \times 10^{18}$  quanta/min). The laser flash photolysis experiments were carried out on an automated setup equipped with pulse Nd laser with  $\lambda = 355$  nm and pulse duration and power being 5 ns and 3.75 mJ, respectively.

The dynamic light scattering spectra were registered on Malvern Zetasizer Nano S at 25 °C. Solutions were illuminated by a He–Ne laser at  $\lambda = 633$  nm; the scattered light registered at an angle of 173°.

### Results and Discussion

Basic hydrolysis of zinc acetate in 2-propanol is a well-studied, reproducible, and comparatively simple method of preparation of colloidal ZnO NPs.<sup>9–11</sup> The same procedure can be also carried out in dry ethanol with two advantages: (i) it produces more concentrated (up to  $2 \times 10^{-2}$  M) zinc oxide colloids as compared with 2-propanol solutions, where ZnO nanoparticles become unstable already at  $[\text{ZnO}] > 2 \times 10^{-3}$  M, and (ii) it allows simple control of the size of ZnO nanoparticles through variations in reagent concentrations.

\* To whom correspondence should be addressed. E-mail: stroyuk@inphyschem-nas.kiev.ua.

<sup>†</sup> L. V. Pysarzhevskiy Institute of Physical Chemistry.

<sup>‡</sup> V. E. Lashkaryov Institute of Semiconductors Physics.

<sup>§</sup> E-mail: dzhagan@isp.kiev.ua.

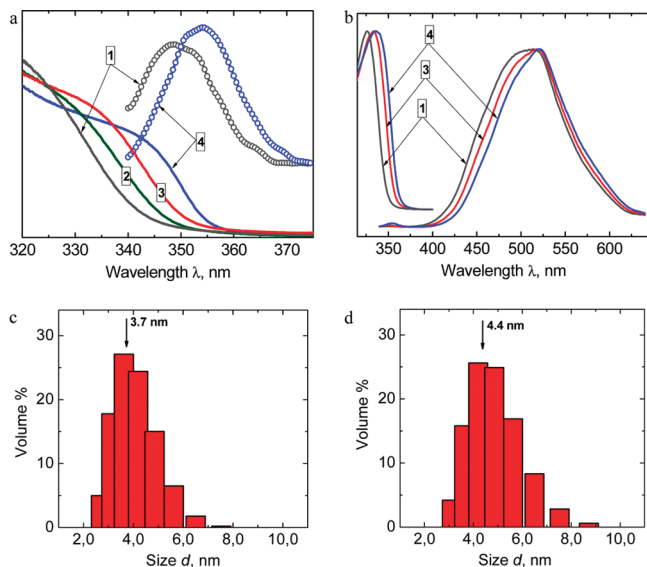


**Figure 1.** (a) Normalized absorption spectra and a section of PL spectra corresponding to excitonic PL for the four samples of ZnO colloids differing in size. (b) Normalized full-size PL and PL excitation spectra of ZnO colloids. The average size of ZnO NPs is 3.7 (1), 3.9 (2), 4.1 (3), and 4.4 nm (4). PL excitation spectra were taken at  $\lambda = 520$  nm. (c, d) Size distribution graphs for the colloidal ZnO solutions synthesized at the initial precursor concentrations  $2 \times 10^{-3}$  (c) and  $2 \times 10^{-2}$  M (d) determined by the dynamic light scattering technique. On c and d the arrows denote the size values derived from the absorption spectra.

**TABLE 1: Spectral Characteristics of ZnO NPs of Different Size**

sample	[ZnO] $\times 10^2$ , M	$\lambda_{tr}$ , nm	$E_g$ , eV	$E_{EPL}$ , eV	$E_{DPL}$ , eV	$d$ , nm
a	0.2	343	3.62	3.55	2.42	3.7
b	0.5	348	3.56	3.54	2.41	3.9
c	1.0	352	3.52	3.52	2.40	4.1
d	2.0	356	3.48	3.48	2.39	4.4

The precursor concentration decrease from  $2 \times 10^{-2}$  to  $2 \times 10^{-3}$  M is accompanied by a “blue” shift of the absorption threshold ( $\lambda_{tr}$ ) of ZnO NPs from 356 to 343 nm (Figure 1a and Table 1) indicating the band gap ( $E_g$ ) of ZnO NPs broadening from 3.48 to 3.62 eV (Table 1). At any given precursor concentration, the band gap of colloidal ZnO NPs is larger than that of bulk ZnO (3.2 eV<sup>12</sup>). This implies that ZnO nanocrystals are in the regime of spatial exciton confinement, where the electronic properties of the semiconductor depend strongly on the NP size  $d$ .<sup>13</sup> In this view, the band gap increase of ZnO NPs is associated with a decrease of  $d$ .

Comparison of the reported experimental data on the relationship between the band gap and the size of ZnO NPs<sup>14,15</sup> with semiempirical  $E_g$ – $d$  correlations derived from various models<sup>14,16–18</sup> showed that the calculation of ZnO NP size in terms of the most popular effective carrier masses approximation, when applied for  $E_g > 3.3$  eV, gives  $d$  values, which are 1–2 nm larger than those determined by X-ray diffraction (XRD) or transmission electron microscopy (TEM) (Figure 2a).

In this connection, to determine the average size of ZnO NPs from absorption spectra, the relationship derived in ref 16 from the 3D exciton model (Figure 2a) appears to be more accurate and agrees well with the experimental data. The estimation showed that the concentration decrease from  $2 \times 10^{-2}$  to  $2 \times 10^{-3}$  M results in the decrease of  $d$  from 4.4 to 3.7 nm (Table 1). The direct measurements of the size of ZnO NPs performed

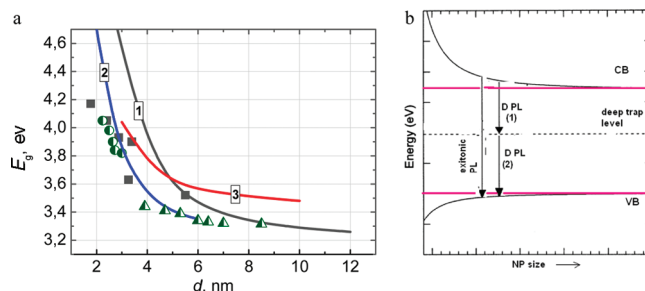


**Figure 2.** (a) Some semiempirical calculations and experimental data (XRD and TEM) on the relationship between the band gap and size of ZnO NPs. The dark-gray line (1) corresponds to the effective carrier masses approximation<sup>26–28</sup> with  $m_e^* = 0.27$  and  $m_h^* = 0.50$ ; the blue line (2) is the result of 3D exciton problem solving;<sup>29</sup> the red line (3) is from use of Kanayama's model with a finite well depth (4.3 eV);<sup>30</sup> black squares and green triangles are XRD measurements;<sup>26,31</sup> green circles are TEM measurements.<sup>26</sup> (b) Scheme illustrating size variation of the energies of optical transitions in ZnO NPs.

in the colloidal solutions of the smallest and highest concentrations (respectively,  $2 \times 10^{-3}$  and  $2 \times 10^{-2}$  M) by the dynamic light scattering method (Figure 1c,d), are in a good correspondence with the estimated values derived from the absorption spectra.

The PL spectra contain a near-band-edge band at  $E_{EPL} = 3.48$ – $3.55$  eV, and a much broader and stronger band peaked at  $E_{DPL} = 2.39$ – $2.42$  eV. The latter PL band is commonly attributed to oxygen vacancies.<sup>7,19–23</sup> As to the near-bandgap PL band, at room temperature it most probably originates from the radiative recombination of free or shallowly trapped excitons.<sup>24</sup>

The excitonic PL band shifts to shorter wavelengths upon NP size decrease, though the shift is smaller (0.07 eV) than that of the absorption edge (0.14 eV). The latter fact can be an indication that at least one of the carriers is shallowly trapped, and the weaker size dependence of the trap energy (compared to the corresponding band edge) results in the observed weak size dependence of the excitonic PL band. Alternatively, even for the “true” excitonic PL, i.e., due to recombination of free electron (e) and hole (h), the increase of Stokes shift with the NP size decrease was reported and associated with the size dependence of the electronic structure of the emitting states in the conduction band (CB).<sup>25</sup>

The visible (deep trap) PL reveals even weaker size dependence of the band position; it shifts only by about 0.03 eV between the 3.7 and 4.4 nm samples (Table 1). Generally, two possible mechanisms for the visible emission can be considered: (1) recombination of a shallowly trapped (delocalized) electron with a deeply trapped hole or (2) recombination of a shallowly trapped hole with a deeply trapped electron (Figure 2b).

The size dependence of the positions of both PL bands can help to distinguish between the two processes. Due to the smaller effective mass of the electron compared to hole, the CB edge depends more strongly on the NP size than the edge of the valence band (VB).<sup>24</sup> As far as the energy level of the deep trap is supposed to be independent of size, the visible PL shift is determined either by CB or VB shift (Figure 2b). On the basis of the visible PL shift being much weaker (0.03 eV) than that of the absorption edge (0.14 eV), the above mechanism 2 can be preferred in our case.

Under illumination of deaerated colloidal solutions of ZnO NPs with the above-bandgap light a noticeable blue shift of both the optical absorption and PL excitation spectra is observed (Figure 3). The shift is completely reversible, and spectra return

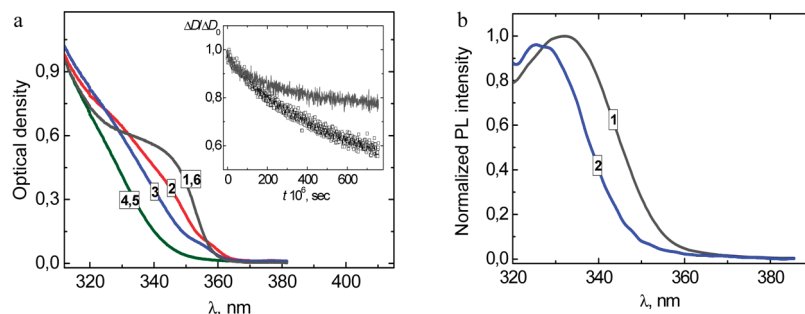


**Figure 3.** Effects of illumination onto the absorption (a) and PL excitation spectra (b) of 4.4 nm ZnO NPs. In a, curve 1 is the initial spectrum. The solution was illuminated by the light source of the luminescence spectrometer for 5 (2) and 10 min (3) and then illuminated by the mercury lamp for 5 (4) and 10 min (5). Curve 6 coincides with 1 and corresponds to the absorption spectrum of the illuminated solution after air admission. In b, curve 1 is the initial PL excitation spectrum and curve 2 is after 5 min illumination by the light source of the luminescence spectrometer. Inset in a: Relaxation of the normalized blue spectral shift (expressed as a photoinduced loss of the optical density at 340 nm,  $\Delta D$ ) of colloidal 3.7 (open squares) and 4.4 nm (solid line) ZnO NPs registered in air-saturated solutions under laser flash illumination at  $\lambda = 340$  nm.  $[\text{ZnO}] = 1.0 \times 10^{-3}$  M.

to their initial positions after the cuvette is opened and the solution is stirred (Figure 3).

On the basis of numerous previous observations of a similar effect on ZnO NP colloids in the presence of a strong hole scavenger (alcohol solvent), we can attribute the observed blue shift of the optical spectra to the filling of the lowest CB states with the photogenerated electrons.<sup>7,19</sup> The complete reversibility of the optical shift excludes any noticeable photodegradation of the NPs during the illumination experiments. Another feature of the blue shift is its saturability. As can be seen from Figure 3, the shift grows with the exposure increase until saturation (spectra 4 and 5 are identical) and then preserves its magnitude for a prolonged time (several hours in the dark).

The accumulation of electrons in the NPs being most probably due to the filling of the lowest CB levels can be evidenced also by an induced absorption at shorter wavelength, around 320 nm (Figure 3). This absorption is obviously an indication of electron excitation to higher CB states due to efficient filling of the lowest states, as has been observed previously for ZnO<sup>7,19</sup> and CdSe<sup>32</sup> NPs. Along with the above evidence of electron charging to delocalized CB states, the fast trapping of electron to the deep states in the band gap can lead to their accumulation at these states as well.<sup>33,34</sup> We will return to this below during discussion of the PL spectra of the illuminated NPs.

The laser flash photolysis experiments both in the air-saturated and bubbled with argon colloidal ZnO solutions showed that the relaxation of the light-induced shift occurs in the micro-millisecond time range, reflecting interaction of the noncompensated electrons with dissolved oxygen and ethanol<sup>34</sup> (Figure 3a, inset). Comparison of the kinetic curves presented in the inset in Figure 3a shows these processes are faster in the case of 3.7 nm NPs as compared with 4.4 nm ZnO NPs. The fact can probably be accounted for by a combination of size effects, specifically, growth of the surface-to-volume ratio with the NP size decrease affecting the dynamics of charge migration and surface trapping, and an increase in the CB energy, estimated to be close to 0.1 eV with the ZnO NP size reducing from 4.4 to 3.7 nm.

The PL spectrum of the ZnO NPs under study changes even more drastically upon illumination (Figure 4) in comparison with the absorption spectrum of the colloidal solution. The most pronounced change is the quenching of deep-trap PL.

The behavior of the deep-trap PL is obviously not governed by the distribution of NP size or trap energies. As opposed to the observations of ref 33, we did not observe any noticeable shift of this band upon quenching; it reduces in intensity without changing its line shape.

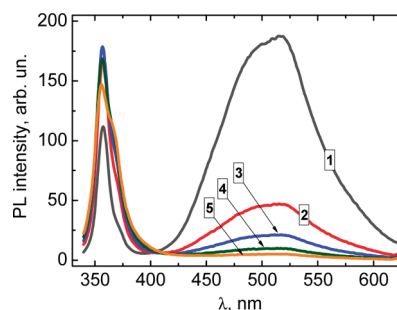


**Figure 4.** Changes of the PL spectrum of 4.4 nm ZnO NPs (curve 1) upon illumination by the light source of the luminescence spectrometer for 1 (curve 2), 4 (3), 10 (4), and 25 min (5).  $[\text{ZnO}] = 1.0 \times 10^{-3}$  M.

The total intensity of the near-bandgap EPL band slightly decreases as well. However, this PL band simultaneously splits into two, with the intensity of the new red-shifted component (denoted as EPL2) increasing in intensity with illumination time (Figures 5 and 6). The synchronous change of two excitonic PL components and the DPL indicates the close connection existing between all the three recombination processes, as will be discussed further.

The new PL feature is more pronounced and grows faster in larger NPs (Figure 5). In the largest NPs (4.4 nm) this feature is already present in the starting PL spectrum, i.e., under the minimum possible illumination time equal to the acquisition time of the starting PL spectrum itself (less than 20 s). In contrast, for the smallest NPs (3.7 nm, sample a), the component was not distinguished even under prolonged illumination, not even a slight broadening of the main PL band could be seen as well.

Some results of fitting and analysis of the excitonic doublet feature are summarized in Figure 7. It shows that both excitonic components shift to shorter wavelengths upon illumination. The width of the new component noticeably increases, while the initial band becomes slightly narrower. All the changes in the PL spectra are, similarly to the absorption and PL excitation, reversible and disappear upon opening of the cuvette and stirring the solution. Moreover, all the effects become order of magnitude weaker when shaking the cuvette before each measurement (Figure 7, open symbols).

On the basis of the experimental data and results of other authors,<sup>7,19,21,23,33</sup> oxygen can be considered to be one of the main factors responsible for the observed changes in the absorbance and PL spectra, first of all, because oxygen is an



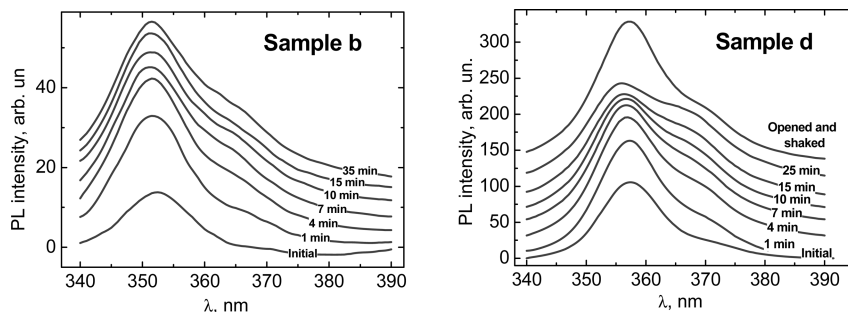


**Figure 5.** Changes of the excitonic PL spectrum of 3.9 (sample b) and 4.4 nm (sample d) ZnO NPs upon illumination by the light source of the luminescence spectrometer.  $[\text{ZnO}] = 1.0 \times 10^{-3} \text{ M}$ .

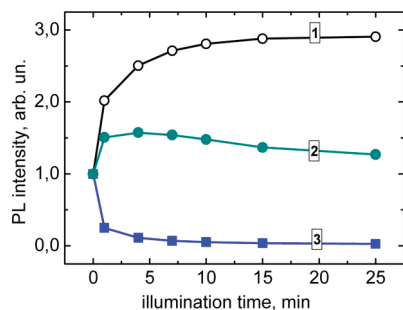


**Figure 6.** Variation of the PL intensity with illumination time for the 4.4 nm ZnO NPs. Curve 1 corresponds to the “new” near-bandgap PL band (EPL2), curve 2 is the total near-bandgap PL intensity, and curve 3 is the DPL intensity.

efficient electron scavenger. If there were an unlimited access of oxygen, as is the case for hole scavenger (ethanol), the optical spectra of the NPs might be in an equilibrium state. However, under deaerated conditions, the traces of oxygen dissolved in the solution are being rapidly depleted (due to their reduction by photogenerated conduction band electrons<sup>33</sup>) and do not withdraw the noncompensated photoexcited electrons, allowing them to accumulate in the semiconductor NP. The process is dramatically slowed by shaking the solution before each measurement due to providing access of remote oxygen molecules in the solution to the NP surface (Figure 7, curve 1). Opening and stirring of the solution opens an unlimited access of oxygen, and solution returns to the initial equilibrium state.

The importance of oxygen in the processes under study is further evidenced by its role established for deep trap emission of ZnO NPs. The intensity of the visible (defect-related) PL has been commonly observed to be reduced under deficiency of oxygen.<sup>7,19,21,23,33</sup> The correlation between the changes in the visible PL intensity, absorption, and the excitonic PL allows one to conclude about the close relation existing between the

presence of oxygen, NPs charging, and appearance of the new excitonic PL band.

The separation between EPL1 and EPL2 bands is about 120 meV. This is well more than the LO phonon energy—70 meV—and much more than the energy of the bound exciton—15 meV. Due to this small binding energy, bound excitons are observed only at low temperatures— $<90 \text{ K}$ .<sup>35</sup>

It was shown previously<sup>33,36,37</sup> that charging of semiconductor NPs leads to a red shift of the luminescence bands. For example, results similar to those reported here were obtained in ref 38 for CdSe NPs where charging-induced bleaching of the first excitonic band and red shift of the excitonic PL band maximum have also been observed. Moreover, in the ensemble with a distribution of NP size, the charging occurs gradually from larger to smaller NPs within the sample.<sup>33</sup> In the present work, this conclusion is supported by the laser flash photolysis results (Figure 3, inset), indicating faster electron withdrawal from smaller ZnO NPs.

Combining these two facts, a model of the present behavior of the excitonic PL under illumination can be suggested. The initial PL band (EPL1) shifts to shorter wavelengths, loses intensity, and narrows due to extraction of the contribution of the largest NPs in the ensemble. The newly arisen and strongly red-shifted EPL2 component is apparently due to the largest NPs getting charged. The criterion for charging is obviously the relative size-dependent positions of the CB and VB levels of ZnO NPs with respect to the reducing (ethanol) and oxidizing ( $\text{O}_2$ ) agents in the solution. As the illumination is continued the portion of charged NPs and the EPL2 band intensity both increase. The simultaneous broadening of the EPL2 band can be in part due to the appearance of the higher-energy ( $\text{P}^{2-}$ ) transition. However, the broadening of the optical spectra of charged NPs is commonly observed even without contribution of the higher-energy transition. The absence of the broadening

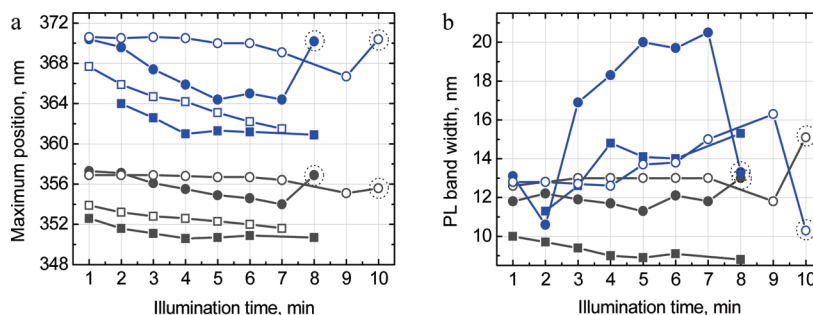


**Figure 7.** Changes of the maximum position (a) and spectral width (b) of EPL1 and EPL2 luminescence bands of ZnO NPs of different size. Dark-gray curves correspond to the EPL1 component; blue, to EPL2. Filled squares, sample b; opened squares, sample c; filled circles, sample d; open circles, sample d shaken after each measurement. The last points, marked by dotted circles, denote the data obtained after the air admission.

for the original EPL1 component can further confirm its assignment to the fraction of smaller NPs which do not get charged.

Our results are in good qualitative agreement with those of Meijerink et al.,<sup>11</sup> where UV-illuminated ZnO NPs in the absence of oxygen revealed drastic quenching of the DPL and an increase of excitonic PL intensity. They observed a red shift of the excitonic emission band as a whole upon illumination and explained it by an increase of emission contribution from the largest NPs which are predominantly charged. Our present results corroborate those of ref 11 and allow the size-selective charging process to be monitored more obviously due to the splitting of the excitonic PL band. Apparently, the bigger ZnO particles can be charged with electrons more easily than the smaller ones due to different rates of noncompensated electrons withdrawal. It has been shown before that the redox potential of quantum-sized ZnO NPs increases with the particle size being reduced.<sup>39</sup> However, the concomitant narrowing of the excitonic band was not commented on in ref 11. The enhancement of the excitonic emission from the NPs with excess electrons in the CB was explained<sup>11</sup> by a higher probability of their recombination with the photogenerated VB holes. This effect is in agreement with the present results. The difference from other works,<sup>40</sup> where charging of the NP via CB filling led to the quenching of excitonic PL, can be explained by a high probability of the Auger process in the experimental conditions of those reports.<sup>40</sup>

Though most of the authors agree upon the DPL of ZnO NPs being mediated by the oxygen vacancy ( $V_O$ ) defect, the divergence still exists concerning the exact mechanism of the recombination. Vanheusden et al.<sup>20</sup> suggested that the “green” emission in ZnO is due to the recombination of electrons in singly occupied oxygen vacancies with the photoexcited holes in the valence band (this corresponds to case 2 in Figure 2b). A recent first-principles calculation by Zhang et al.<sup>41</sup> supports this identification and shows that  $V_O$  defects have low formation enthalpy and hence are readily produced. The photogenerated electrons can be trapped into oxygen vacancies through a nonradiative decay and then recombine with the VB holes, emitting PL quanta in the visible region. On the other hand, many other experimental results indicate recombination of the free or shallowly trapped electron with a deeply ( $\sim 1$  eV) trapped hole<sup>7,21–23,33</sup> (mechanism 1 in Figure 2b). It is unlikely to identify which of the recombination mechanisms dominate in the present work. On the one hand, the weak size dependence of the DPL (Table 1) band favors the former recombination mechanism (process 2 in Figure 2b). Those reports where mechanism 1 was accepted revealed much stronger dependence of the DPL band position upon the NP size,<sup>24</sup> in agreement with strong size dependence of the CB edge. On the other hand, the PL behavior in the present study of illumination and oxygen effects is in strong agreement with the majority of works where recombination of the free or shallowly trapped electron with a deeply ( $\sim 1$  eV) trapped hole was deduced.<sup>7,21–23,33</sup> The large variation of both the DPL band position and width (up to 0.5 eV) among different studies can be an indication of its multicomponent structure as well as of the complex structure of the underlying energy levels.

## Conclusions

We have investigated the evolution of optical absorption and emission spectra for a series of colloidal ZnO nanoparticles subjected to the above-bandgap photoexcitation. The reversible shifts of the absorption and PL excitation spectra have been

observed, indicating charging of the nanoparticles with photo-excited electrons. The results of laser flash photolysis have shown the consumption of the noncompensated electron in reactions with the solution components (oxygen, solvent) is faster for 3.7 nm ZnO NPs than for 4.4 nm particles.

A rapid drop of deep-level PL band intensity at an early stage of illumination is observed simultaneously with the splitting-off and growth of a new red-shifted near-band-edge PL band. Such a splitting of the near-bandgap PL band under illumination is observed for the first time. The possible relation between the new PL band and photoinduced charging of NPs with excess electrons is discussed in terms of the dependence of the PL spectrum on the NP size and controllable access of oxygen during illumination.

**Acknowledgment.** We appreciate the help of Prof. Victor F. Plysnin (Institute of Chemical Kinetics and Combustion of the Siberian Branch of Russian Academy of Sciences, Novosibirsk, Russia) in the laser flash photolysis experiments, and thank Dr. Andriy G. Derzhypolskiy (Research Center “ALT-Ukraine LTD”, Kyiv, Ukraine) for the dynamic light scattering measurements.

## References and Notes

- (1) Djurii, A. B.; Leung, Y. H. *Small* **2006**, *2*, 944.
- (2) Gao, W.; Li, Z. *Int. J. Nanotechnol.* **2009**, *6*, 245.
- (3) Look, D. C. *J. Electron. Mater.* **2006**, *35*, 1299.
- (4) Fonoberov, V. A.; Alim, K. A.; Balandin, A. A.; Xiu, F.; Liu, J. *Phys. Rev. B* **2006**, *73*, 165317.
- (5) Erwin, S. C.; Zu, L.; Haftel, M. I.; Efros, A. L.; Kennedy, T. A.; Norris, D. J. *Nature* **2005**, *436*, 91.
- (6) Guyot-Sionnest, P. *Microchim. Acta* **2008**, *160*, 309.
- (7) Shim, M.; Guyot-Sionnest, P. *J. Am. Chem. Soc.* **2001**, *123*, 11651.
- (8) Stroyuk, A. L.; Shvalagin, V. V.; Kuchmiy, S. Ya. *J. Photochem. Photobiol. A* **2005**, *173*, 185.
- (9) Bahnmann, D. W.; Kormann, C.; Hoffmann, M. R. *J. Phys. Chem.* **1987**, *91*, 3789.
- (10) Bahnmann, D. W. *Isr. J. Chem.* **1993**, *33*, 115.
- (11) van Dijken, A.; Meulenkaamp, M. A.; Vanmaekelbergh, D.; Meijerink, A. *J. Phys. Chem. B* **2000**, *104*, 4355.
- (12) Wu, F.; Yu, J.; Joo, J.; Hyeon, T.; Zhang, J. *Opt. Mater.* **2007**, *29*, 858.
- (13) Vossmeier, T.; Katsikas, L.; Giersig, M.; Popovic, I.; Diesner, K.; Chemseddine, A.; Eychmüller, A.; Weller, H. *J. Phys. Chem.* **1994**, *98*, 7665.
- (14) Nandakumar, P.; Vijayan, C.; Mutri, Y. *J. Appl. Phys.* **2002**, *91*, 1509.
- (15) Brus, L. *J. Chem. Phys.* **1984**, *80*, 4403.
- (16) Baskoutas, S.; Terzis, A. *J. Appl. Phys.* **2006**, *99*, 013708.
- (17) Matsumoto, H.; Sakata, T.; Mori, H.; Yoneyama, H. *J. Phys. Chem.* **1996**, *100*, 13781.
- (18) Nanda, K.; Kruis, F.; Fissan, H. *Nano Lett.* **2001**, *1*, 605.
- (19) Kamat, P. V.; Patrick, B. *J. Phys. Chem.* **1992**, *96*, 6829.
- (20) Vanheusden, K.; Warren, W. L.; Seager, C. H.; Tallant, D. R.; Voigt, J. A.; Gnade, B. E. *J. Appl. Phys.* **1996**, *79*, 7983.
- (21) van Dijken, A.; Meulenkaamp, E. A.; Vanmaekelbergh, D.; Meijerink, A. *J. Phys. Chem. B* **2000**, *104*, 1715.
- (22) Koch, U.; Fojtik, A.; Weller, H.; Henglein, A. *Chem. Phys. Lett.* **1985**, *122*, 507.
- (23) Bohle, D. S.; Spina, C. J. *J. Am. Chem. Soc.* **2007**, *129*, 12380.
- (24) van Dijken, A.; Meulenkaamp, E. A.; Vanmaekelbergh, D.; Meijerink, A. *J. Lumin.* **2000**, *90*, 123.
- (25) Demchenko, D. O.; Wang, L.-W. *Phys. Rev. B* **2006**, *73*, 155326.
- (26) Wood, A.; Giersig, M.; Hilgendorff, M.; Vilas-Campos, A.; Liz-Marzán, L. M.; Mulvaney, P. *Aust. J. Chem.* **2003**, *56*, 1051.
- (27) Wong, E. M.; Hoertz, P. G.; Liang, C. J.; Shi, B.-M.; Meyer, G. J.; Searson, P. C. *Langmuir* **2001**, *17*, 8362.
- (28) Pesika, N. S.; Hu, Z.; Stebe, K. J.; Searson, P. C. *J. Phys. Chem. B* **2002**, *106*, 6985.
- (29) Fonoberov, V. A.; Balandin, A. A. *Phys. Rev. B* **2004**, *70*, 195410.
- (30) Monticone, S.; Tufeu, R.; Kanaev, A. V. *J. Phys. Chem. B* **1998**, *102*, 2854.
- (31) Wang, Y. S.; Thomas, P. J.; O'Brien, P. J. *J. Phys. Chem. B* **2006**, *110*, 4099.
- (32) Shim, M.; Guyot-Sionnest, P. *Nature* **2000**, *407*, 981.

- (33) Yanhong, L.; Dejun, W.; Qidong, Z.; Min, Y.; Qinglin, Z. *J. Phys. Chem. B* **2004**, *108*, 3202.
- (34) Wood, A.; Giersig, M.; Mulvaney, P. *J. Phys. Chem. B* **2001**, *105*, 8810.
- (35) Peng, W. Q.; Qu, S. C.; Cong, G. W.; Wang, Z. G. *Appl. Phys. Lett.* **2006**, *88*, 101902.
- (36) Houtepen, A. J.; Vanmaekelbergh, D. *J. Phys. Chem. B* **2005**, *109*, 19634.
- (37) Franceschetti, A.; Zunger, A. *Phys. Rev. B* **2000**, *62*, 16287.
- (38) Wang, C.; Wehrenberg, B. L.; Woo, C. Y.; Guyot-Sionnest, P. *J. Phys. Chem. B* **2004**, *108*, 9027–9031.
- (39) Hoyer, P.; Weller, H. *Chem. Phys. Lett.* **1993**, *221*, 479.
- (40) Shim, M.; Wang, C.; Guyot-Sionnest, P. *J. Phys. Chem. B* **2001**, *105*, 2369.
- (41) Zhang, S. B.; Wei, S.-H.; Zunger, A. *Phys. Rev. B* **2001**, *63*, 075205.

JP908879H